

Journal of Advanced Scientific Research

ISSN

0976-9595

Research Article

Available online through http://www.sciensage.info

STRUCTURAL, OPTICAL AND PHOTOCATALYTIC STUDIES OF ANATASE-RUTILE MIXED-PHASE UNDOPED AND SILVER-DOPED TITANIUM DIOXIDE NANOPARTICLES

T. Sunitha¹, C. Gnanasambandam², K. Monikanda Prabu³*

¹Research Scholar (Reg. No.- 12110), Physics Research Centre , S.T. Hindu College, Nagercoil, Manonmaniam Sundaranar University, Tirunelveli, Tamilnadu, India

²Department of Physics, S.T. Hindu College, Nagercoil, Manonmaniam Sundaranar University, Tirunelveli, Tamilnadu, India ³Physics Research Centre, S.T. Hindu College, Nagercoil, Manonmaniam Sundaranar University, Tirunelveli, Tamilnadu, India. *Corresponding author: mkprabu1985@gmail.com

ABSTRACT

Undoped and silver-doped titanium dioxide (TiO_2) nanoparticles are prepared by the Sol-Gel process using Titanium isopropoxide (TTIP) as a precursor. The synthesized nanoparticles are characterized by powder X-ray diffraction (PXRD), Fourier transform infrared spectroscopy (FT-IR), UV-VIS spectroscopy and photocatalytic studies. The powder X-ray diffraction characterization results showed that the thermal treatment at 500 °C leads to the formation of anatase-rutile mixed phase TiO_2 nanoparticles. The formation of TiO_2 nanoparticles is also confirmed from the dominant FT-IR peaks observed below 650 cm⁻¹. The UV-VIS spectroscopy shows that the silver-doping causes narrowing the optical band gap value of \sim 2.89 eV. Photocatalytic investigation shows that the silver-doping leads to higher degradation efficiency of 86.35%.

Keywords: Titanium dioxide, Silver-doping, Optical properties, Photocatalysis

1. INTRODUCTION

dioxide a well-known semiconducting nanomaterial found major applications in the field of photocatalysis [1]. TiO₂ exist in three polymorphs namely, anatase, rutile and brookite. Due to the large bandgap (~3.2 eV) values of these three crystallographic forms their potential applications excellent only in the UV region [2]. The major factor which affects the photocatalytic efficiency is rapid recombination of photogenerated electron-hole pairs [3]. One of the effective ways for splitting-up of this photogenerated electron-hole pair is doping with silver ions [4]. Numerous methods such as ball-milling [5], combustion method [6], microwave method [7], solvothermal method [8], hydrothermal method [9], and sol-gel method [10] have been adapted to synthesize silver doped TiO₂nanoparticles. Among these methods, the sol-gel process is the most promising technique for synthesizing silver-doped TiO2nanoparticles.In this paper, nanosized undoped and silver-doped TiO2 nanoparticles are prepared by the sol-gel technique. The structural properties of the nanosized undoped and silver-doped TiO₂nanoparticles are characterized by PXRD and FT-IR. The optical property of these samples was investigated by UV-VIS Kubelka-Munk absorption. The photocatalytic efficiency of undoped and silver-doped ${\rm TiO_2}$ nanoparticles are investigated by the photodegradation of methyl orange (MO) solution under visible light illumination.

2. EXPERIMENTAL

2.1. Materials

Titanium tetra-isopropoxide (TTIP, 97%, Sigma Aldrich), Ethanol (RANKEM), Deionized water, Silver Nitrate (Merck).

2.2. Preparation of TiO₂Nanoparticles

Undoped and silver-doped ${\rm TiO_2}$ nanoparticles are prepared by the simple sol-gel route by using the precursor TTIP and deionized water. In this procedure, 10 ml of deionized water is added to 100 ml of ethanol taken in a beaker under room temperature. The mixed solution is stirred well up for ten minutes. Now the pH of the solution is adjusted in the acid range by using nitric acid. Then 15 ml of TTIP is added dropwise to the above mixed solution. While adding TTIP hydrolysis reaction takes place and the ${\rm TiO_2}$ nanoparticles are obtained in the form of a gel in the beaker. The gel is filtered, dried, powdered and calcinated to 500 °C. For the silver-doping

suitable amount of doping material (1 wt% Ag⁺) is added to the water and dissolves before mixed with ethanol.

2.3. Characterization

The synthesized undoped and silver-doped TiO_2 nanoparticles are characterized by various sophisticated techniques. Powder X-ray diffraction (PXRD) spectra are recorded by using XPERTPRO diffractometer with diffraction angle 2θ in the range $10\text{-}80^\circ$ using Cu-K α radiation of wavelength 1.54060 Å. FTIR spectra are recorded by using BRUKER-TENSOR 27 model FTIR instrument. UV-VIS diffuse reflectance spectra are carried out by using the VARIANCary 500 Scan model spectrometer.

2.4. Photocatalytic activity

The photocatalytic activity of undoped and silver-doped TiO₂ nanoparticles are evaluated by checking over the degradation of azo dye methyl orange (MO) under visible light (18 W, fluorescent lamp) excitation. For this typical study, 50 ml of 10 ppm aqueous MO solution is taken in a 100 ml beaker. 0.1 g of undoped and silver-doped powdered TiO₂ nanoparticles are dispersed separately in this solution. The solution is irradiated with UV light up to 210 min. Every 30 min, 5 ml of MO solution is taken out and is centrifuged immediately to remove the catalyst. The degradation efficiency of undoped and silver-doped TiO2nanoparticles is viewed through UV-Vis absorption spectra of MO solution. The standard curve between concentration and absorption, the value of $((C_0-C_t/C_0) \times 100\%)$ is calculated, signified as the degradation percentage. Figure (1) shows the image of the photocatalytic experimental reactor.

- 1. Fluorescent lamp
- 2. MO solution
- 3. Stand

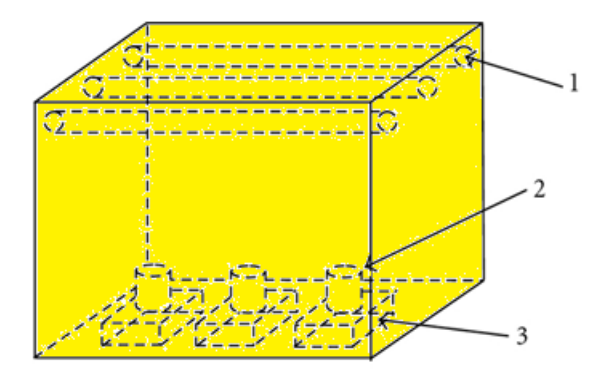


Fig.1: Image of the Photocatalytic Experimental Reactor

3. RESULTS AND DISCUSSION

3.1. Powder X-ray diffraction Analysis

Figures (2&3) show the PXRD patterns of undoped and silver-doped ${\rm TiO_2}$ nanoparticles. The peaks are very sharp which specifies that the crystallinity is increased due to calcination. Both the spectra shows anatase-rutile mixed-phase ${\rm TiO_2}$ with high-intensity peaks of rutile and lower intense peaks of anatase phase.

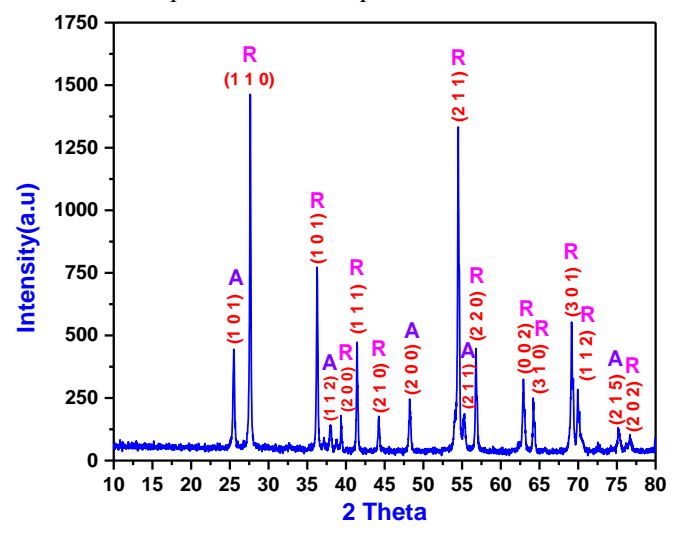


Fig. 2: PXRD pattern of undoped TiO₂ nanoparticles

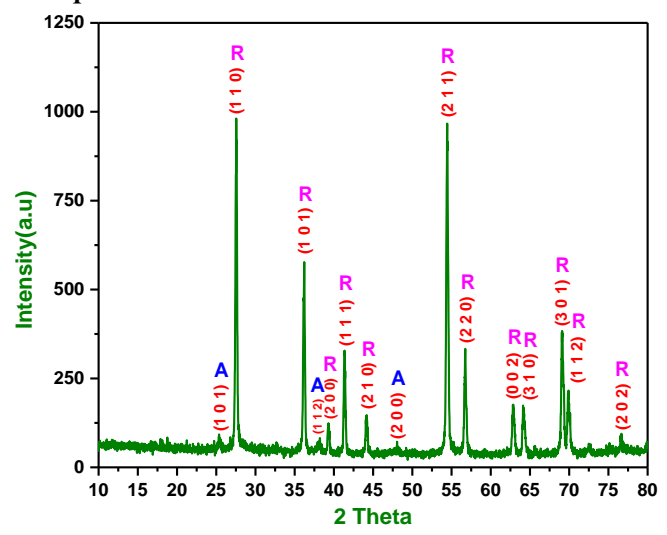


Fig.3: PXRD pattern of silver-doped TiO₂ nanoparticles

The spectrum of undoped TiO_2shows twelve peaks appears at 2θ values 27.63, 36.27, 39.38, 41.43, 44.21, 54.49, 56.80, 62.91, 64.25, 69.13, 69.94, and 76.68 are nominated as (1 1 0), (1 0 1), (2 0 0), (1 1 1), (2 1 0), (2 1 1), (2 2 0), (0 0 2), (3 10), (3 0 1), (1 1 2), and (2 0 2) planes of rutile phase, respectively. Furthermore, The spectrum of silver-doped TiO_2shows twelve peaks exist at 2θ angles at 27.57, 36.22, 39.26, 41.36, 44.13,

54.45, 56.74, 62.82, 64.16, 69.07, 69.86and 76.59 are corresponding to the planes of rutile phase(1 1 0), (1 0 1), $(2\ 0\ 0)$, $(1\ 1\ 1)$, $(2\ 1\ 0)$, $(2\ 1\ 1)$, $(2\ 2\ 0)$, $(0\ 0\ 2)$, $(3\ 1\ 1)$ 0), (3 0 1),(1 1 2),and (2 0 2), respectively [11]. The undoped TiO2 spectrum shows five characteristic diffraction peaks of anatase about 2θ values at 25.50, 48.24, 55.32, and 75.23, which are corresponding to the Miller indices of planes (1 0 1), (1 1 2), (2 0 0), (2 1 1), and (2 1 5), respectively. The silverdoped TiO₂ spectrum shows three characteristic diffraction peaks of anatase about 2θ values at 25.41, 38.11, and 47.81 are assigned to the Miller indices of planes (1 0 1), (1 1 2), and (2 0 0), respectively [12]. Moreover, in the case of silver-doped TiO₂ spectrum the peaks of anatase are suppressed which suggests that the doping with silver ions promote the phase transformation from anatase to rutile at lower temperature calcination which agrees with the previous findings of silver-doped TiO₂nanoparticles [13]. The fraction of anatase-rutile is determined by the Spurr-Myers equation [14],

$$W_{A} = 100 / (1+1.265 I_{R}/I_{A})$$

$$W_{R} = 100 / (1+0.8 I_{A}/I_{R})$$
(1)
(2)

$$W_{R} = 100 / (1 + 0.8 I_{A} / I_{R})$$
 (2)

Where, W_R and W_A are the weight percentage of rutile and anatase. I_A is the intensity of anatase peak and I_R is the intensity of rutile peak. For undoped TiO₂nanoparticles the anatase-rutile weight calculated from the above relation is 18:72, and for silver-doped TiO₂nanoparticles, it is found to be 3:97. The average crystallite size of the undoped and silverdoped TiO2nanoparticlesis determined by the familiar Scherrer formula [15, 16],

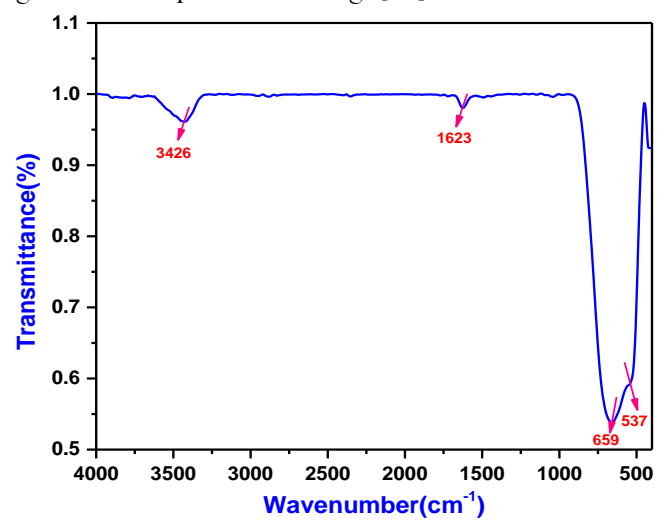
$$C_{A} = 0.9\lambda / \beta \cos\theta \tag{3}$$

Where C_A is the average crystallite size, λ is the wavelength of X-ray, β is the full-width half maximum (FWHM) and θ is the Bragg's angle of diffraction. The crystallite size obtained from the above formula is 54 and 60 nm for undoped anatase and rutile phase TiO₂ nanoparticles, respectively. Which is calculated from the (1 0 1) plane of anatase and (1 1 0) plane of rutile phases, correspondingly. For silver-doped TiO2nanoparticles, it is estimated at 40 and 70 nm for anatase and rutile phase, respectively. Moreover, the ionic radius of Ag⁺ion (1.26) Å) is much larger than Ti⁴⁺ion(0.74Å) as a consequence that the silver ions cannot replace the Ti⁴⁺ions.Hence,

the silver ions are distributed on the surface of TiO₂ [17-

3.2. FT-IR Analysis

Figure (4) shows the FT-IR spectrum of undoped TiO, nanoparticles. The spectrum displays two low intense peaks located at 3426 and 1623 cm⁻¹ the former is assigned to surface adsorbed water and later is assigned to O-H group. In addition to this, the spectrum flashes two high-intensity peaks exist at 659 and 537 cm⁻¹ which is attributed to stretching modes of Ti-O bonds [21-23]. The silver-doped FT-IR spectrum (Figure (5)) have been seemed to be identical bands with a slight shift in peak positions. The peaks appear below 650 cm⁻¹ are assigned to Ti-O and Ag-O vibrations [24]. These assessments agree with the previous findings [25].



4: **FT-IR** spectrum of undoped TiO, nanoparticles

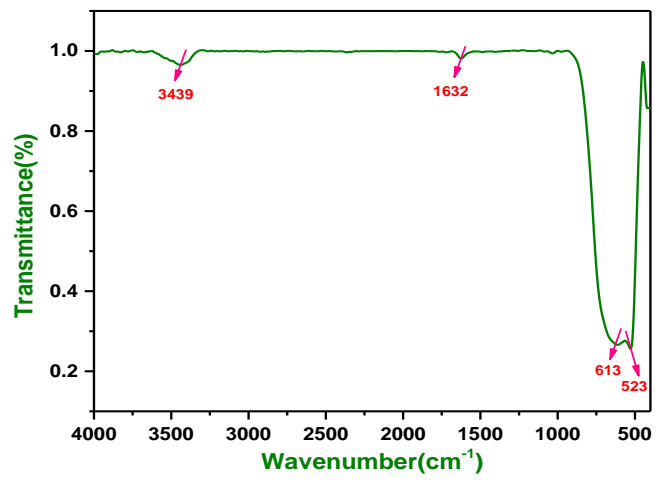


Fig. 5: FT-IR spectrum of silver-doped TiO₂ nanoparticles

3.3. UV-VIS spectral Analysis

In order to examine the optical band gap of the synthesized undoped and silver-doped TiO₂ nanoparticles diffuse reflectance spectral studies in the UV-VIS region is performed.

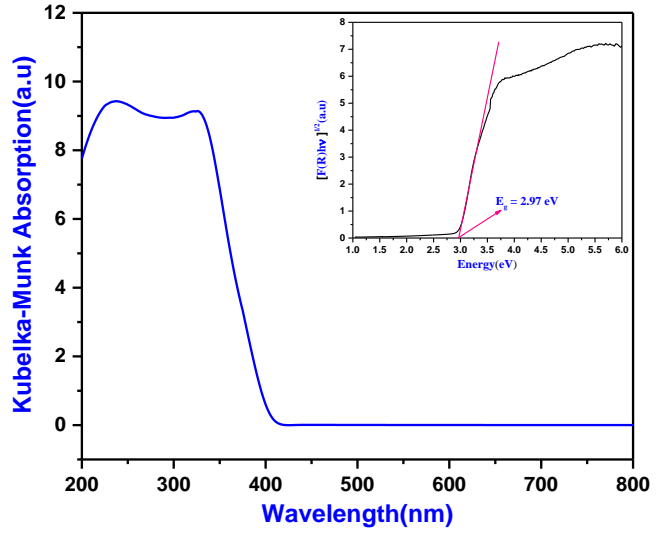


Fig. 6: UV-VIS Kubelka-Munk absorption spectrum of undoped TiO₂nanoparticles (Inner graph - corresponding Tauc Plot)

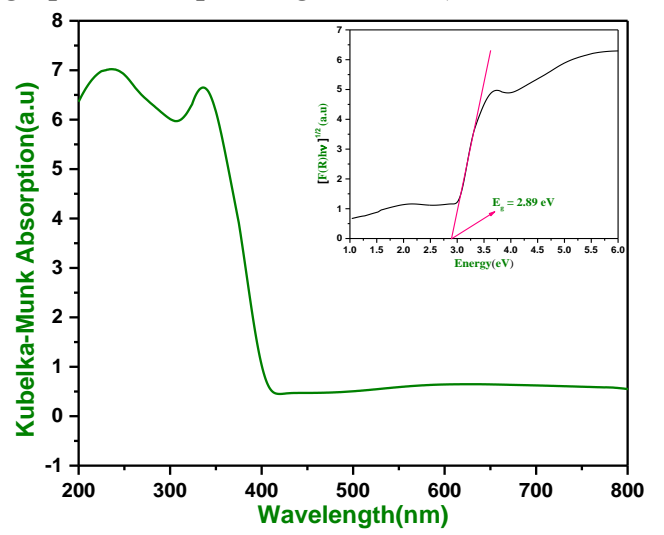


Fig. 7: UV-VIS Kubelka-Munk absorption spectrumof silver-doped TiO₂nanoparticles (Inner graph - corresponding Tauc Plot)

The diffuse reflectance spectrum is transformed into the Kubelka-Munk absorbance F(R) by using the relation [26],

$$F(R) = (1-R)^2 / 2R (4)$$

The optical band gap value of undoped and silver-doped TiO_2 nanoparticles are evaluated from the Tauc's relationship [27-31],

$$[F(R)hv]^{n} = B (hv-E_{\sigma})$$
 (5)

Where hv is the energy of the photon, B is the constant of proportionality, and n is the constant, which depends on the nature of the optical transition. The value of n is $\frac{1}{2}$ for the indirect optical transition. Assuming the indirect band gap and plotting the graph between $[F(R) hv]^{1/2}$ and hv along y and x-axis gives the Tauc plot. To determine the optical band gap from the graph a line is drawn from the maximum slope of the curve to the hv axis at $[F(R) hv]^{1/2}=0$ gives the value of indirect band gap.

For undoped TiO₂ nanoparticles, the band gap value obtained from Tauc plot is 2.97 eV. The optical absorption edge shifted to red light zone for silver-doped TiO₂ nanoparticles correspondingly the reduction in the optical band gap is observed, which is equal to 2.89 eV.

3.4. Investigation of Photocatalytic Efficiency

The photocatalytic efficiency of the undoped and silver-doped TiO₂ nanoparticlesis investigated under visible light using an azo-dye MO as a model pollutant.

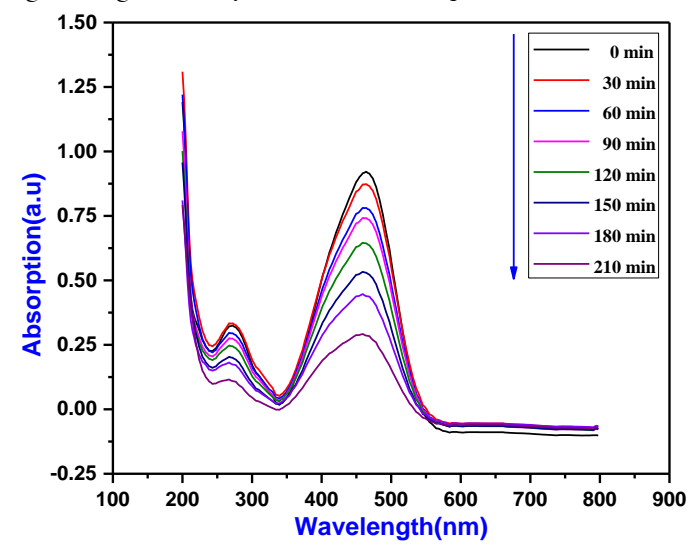


Fig. 8: Decolourisation of MO solution vs. Time in a typical photocatalytic experiment with undoped TiO₂performed under visible light irradiation

Figures 8 & 9 show the decolourisation of MO under visible light irradiation with undoped and silver-doped ${\rm TiO_2}$, respectively. The photocatalytic degradation efficiency of undoped and silver-doped ${\rm TiO_2}$ nanoparticles is shown in figure 10. The silver-doped ${\rm TiO_2}$ shows the photocatalytic efficiency of 86.35%, which is greater than the photocatalytic efficiency of undoped ${\rm TiO_2}$ (68.29%).

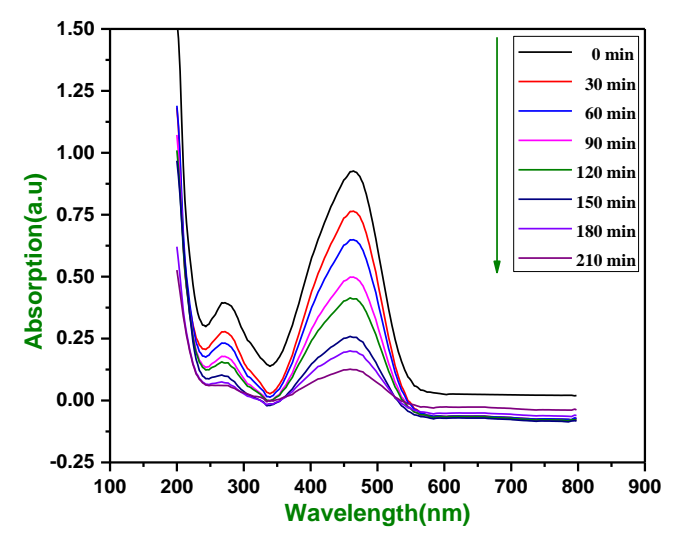


Fig. 9: Decolourisation of MO solution vs. Time in a typical photocatalytic experiment with silver-doped TiO₂performed under visible light irradiation

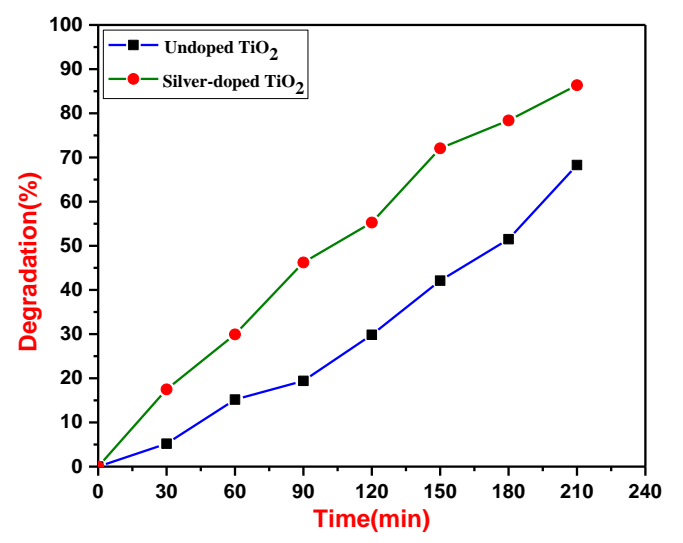


Fig. 10: Photocatalytic degradation efficiency of undoped and silver-doped TiO₂ nanoparticles

This improvement in photocatalytic activity is explained as follows. On account of illumination of TiO_2 nanoparticles with visible light of energy greater than or equal to the bandgap, an electron from the valence band excited to the conduction band and generates electronhole pairs. The lifetime of these charge carriers is very short, so they are recombined instantly thereby by reducing the photocatalytic activity. Herein, PXRD result suggests that the silver ions are adsorbed on the surface of TiO_2 . It follows that the silver ions act as a trapping site and capture the photogenerated electrons thereby inhibits the electron-hole pair recombination. Further, these electrons and holes produce superoxide (O_2^{\leftarrow}) and hydroxyl (OH^{\bullet}) radicals which react with the

water and degrade the MO solution efficiently [32-34]. Hence, the photocatalytic efficiency is more for silver-doped ${\rm TiO_2}$ nanoparticles than undoped ${\rm TiO_2}$ nanoparticles.

4. SUMMARY AND CONCLUSION

The undoped and silver-doped TiO2nanoparticles are successfully synthesized by the simple sol-gel technique. Anatase-rutile mixed phase TiO2nanoparticles are obtained after annealing to 500 °C. PXRD results suggest that the silver-ions are located on the surface of TiO₂due to larger ionic radius than Ti⁴⁺. The FT-IR result indicates that the Ti-O and Ag-O vibrations have strongly appeared below 650 cm⁻¹. The UV-VIS spectral studies show that the absorption edge is red shifted for silverdoped TiO, nanoparticles. The silver-doped TiO, shows higher photocatalytic efficiency than undoped TiO₂. The presence of silver ions on the surface of TiO₂retards there combination rate of electron-hole pairs. Hence, the separation of charge carriers enhanced thereby increasing the photocatalytic efficiency of silver-doped TiO, nanoparticles. In conclusion, silver-doped TiO, nanoparticles are the effective photocatalysis than undoped TiO₂ nanoparticles for completely decolorizing azo-dyes.

5. REFERENCES

- Harikishore M, Sandhyarani M, Venkateswarlu K, Nellaippan TA, Rameshbabu N, *Proc. Mater. Sci.*, 2014; 6:557-566
- 2. Alsharaeh EH, Bora T, Soliman A, Ahmed F, Bharath G, Ghoniem MG, Abu-Salah KM, Dutta J, *Catalysts.*, 2017; 133(7):1-10
- 3. Schneider J, Matsuoka M, Takeuchi M, Zhang J, Horiuchi Y, Anpo M, Bahnemann DW, *Chem. Rev.*, 2014;**114(9)**:9919-9986
- 4. Santos LM, Machado WA, Franca MD, Borges KA, Paniago RM, Patrocinio AOT, Machado AEH, RSC Adv., 2015; 5:103752-103759
- 5. Aysin B, Ozturk A, Park J, Ceramic. Inter., 2013; **39**: 7119-7126
- 6. Kitamura Y, Okinaka N, Shibayama T, Mahaney OOP, Kusano D, Ohtani B, Akiyama T, *Powder*. *Tech.*, 2007; **176**:93-98
- 7. Suwarnkar MB, Dhabbe RS, Kadam AN, Garadkar KM, Ceramic. Inter., 2014; 40:5489-5496
- 8. Naghibi S, Gharagozlou M, J. Chin. Chem. Soc., 2017; **64(6)**: 640-650
- 9. Lazau C, Sfirloaga P, Orha C, Ratiu C, Grozescu I, *Mater. Lett.*, 2011; **65**:337-339

- Mogal SI, Gandhi VG, Mishra M, Tripathi S, Shripathi T, Joshi PA, Shah DO, Ind. Eng. Chem. Res., 2014; 53:5749-5758
- 11. Selman AM, Husham M, Sens. Bio-Sens. Res., 2016; 11:8-13
- 12. Li J, Chen X, Ai N, Hao J, Chen Q, Strauf S, Shi Y, *Chem. Phy. Lett.*, 2011; **514**:141-145
- 13. Gupta K, Singh RP, Pandey A, Pandey A, Beilstein J. Nanotechnol., 2013; 4:345-351
- 14. Saravy HI, Safari M, Darban AK, Rezaei A, *Anal. Lett.*, 2014; **47(10)**:1772-1782
- 15. Karkare MM, IEEE. ICACACT., 2014
- 16. Lima FM, Martins FM, Junior PHFM, Almeida AFL, Freire FNA, *Rev. Mater.*, 2018; **23(1)**:1-9
- 17. Yu J, Xiong J, Cheng B, Liu S, A. Catal. B: Envir., 2005; **60**:211-221
- 18. Castro CA, Jurado A, Sissa D, Giraldo SA, *Int. J. Photo.*, 2012; **261045**:1-10
- 19. Pham TD, Lee BK, Chem. Eng. J., 2017; 307:63-73
- 20. Shayegan Z, Lee CS, Haghighat F, Chem. Eng. J., 2018; 334:2408-2439
- 21. Benito HE, Sanchez TDA, Alamilla RG, Enriquez JMH, Robles GS, Delgado FP, *Braz. J. Chem. Engi.*, 2014; **31(3)**:737-745
- 22. Kaur M, Verma NK, J. Mater. Sci. Technol., 2014; **30(4)**:328-334

- 23. Rajamannan B, Mugundan S, Viruthagiri G, Praveen P, Shanmugam N, Spec. Acta. Part A: Mol. Bio. Spec., 2014; 118:651-656
- 24. Kumar B, Smita K, Angulo Y, Cumbal L, *Green Proc. Synth.*, 2016; **5**:371-377
- 25. Yuan Y, Ding J, Xu J, Deng J, Guo J, J. Nano. Nanotech., 2010; **10**:4868-4874
- 26. Lin H, Huang CP, Li W, Ni C, Shah SI, Tseng YH, *App. Catal. B: Environ.*, 2006; **68**:1-11
- 27. Kisch H, Sakthivel S, Janczarek M, Mitoraj D, *J. Phys. Chem. C.*, 2007; **111**:11445-11449
- 28. Ganesh I, Kumar PP, Gupta AK, Sekhar PSC, Radha K, Padmanabham G, Sundararajan G, *Proc. App. Cera.*, 2012; **6(1)**:21-36
- 29. Loan TT, Long NN, VNU J. Sci. Math. Phy., 2014; 30(2):59-67
- 30. Mostaghni F, Abed Y, Mater. Res., 2016; 0191
- 31. Tsega M, Dejene FB, Heliyon., 2017; 3:e00246
- 32. Nainani R, Thakur P, Chaskar M, *J. Mater. Sci. Eng. B.*, 2012; **2(1)**:52-58
- 33. Kumar R, Rashid J, Barakat MA, *Col. Inter. Sci. Comm.*, 2015; **5:**1-4
- 34. Chaker H, Aouali LC, Khaoulani S, Bengueddach A, Fourmentin S, *J. Photo. Photobiol. A: Chem.*, 2016; 318:142-149